



MSc Advanced Manufacturing Technology & System Management (AMT)

Assessment 2

Finite Element Analysis (FEA) of Lathe Parting tool Using Ansys

Supervisor: Dr. Lee Margetts

Date of Submission: 29/11/2021

Project Team Member Name:

**10865308 Yoon Won Jang
10888135 Jinqiao Li
10844253 Zien Zheng
10670077 Jiawen Fan**

PROJECT TITLE	Finite Element Analysis (FEA) of Lathe Parting tool using Ansys
PROJECT TEAM	Yoon Won Jang, 10865308, AMT
	Jinqiao Li, 10888135, AMT
	Zien Zheng, 10844253, AMT
	Jiawen Fan, 10670077, AMT

1. ANALYSIS SPECIFICATION

1.1 PURPOSE OF THE ANALYSIS

Parting tool is widely used for metal cutting operations (Madireddy, 2014) as a part of a lathe machine. However, during operation, a parting tool experiences huge shearing forces (Camuz, S. et al., 2018) which would occur directional deformation of a tool. Therefore, FEA under both idealised and realistic conditions is carried out to help quantify a deflection of the chosen tools and compare the results in this paper.

1.2 TYPE OF ANALYSIS

We selected static structural analysis with the linear and elastic relationship between stress and strain. In addition, materials are assumed to be isotropic. Comparative deflection analysis of parting tool could give an idea when engineers need to select proper material or condition since the static analysis can be conducted to investigate the structural condition such as deformation, stress, and others with the range of loading (EnterFEA, 2019).

1.3 SELECTION OF ELEMENT TYPE

Theoretically, with the same number of elements, the hexahedral mesh would be more accurate than tetrahedral mesh since it has more degrees of freedom when the model is simple enough with few distortions. Therefore, the 3D solid quadratic hexahedral mesh is used for the analysis. Moreover, according to Steven E. Benzley et al., the quadratic hexahedral mesh has brought more accurate results than other types of mesh (Benzley et al., 1995).

1.4 IDEALISATION OF THE PROBLEM

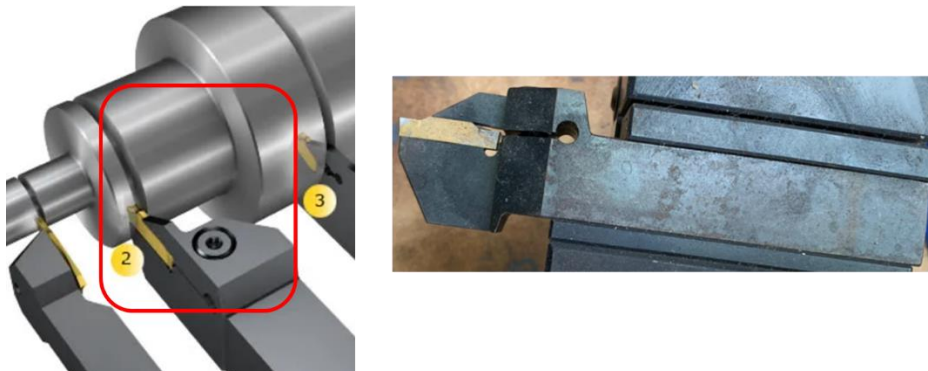


figure 1 The real engineering process and real parting tool

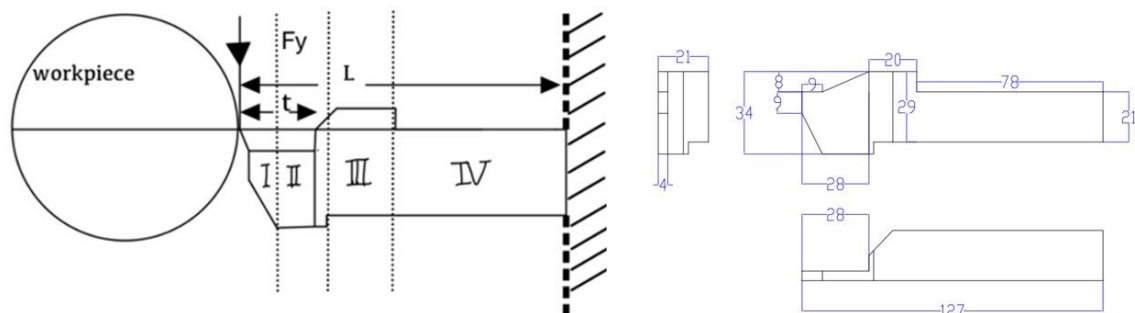


figure 2 The sketch of the idealisation and simplified geometry of parting tool

The figure 1 indicates the image of the lathe parting process and the real parting tool. For the analysis, we simplified the model and the process as figure 2. Only the tangential force is applied to the tip of the tool and the end of the tool is constrained by the fixed support. Moreover, the tool is divided into 4 different sections, and dimensions are shown in the figure.

1.5 SELECTION OF THE BOUNDARY CONDITIONS

The tool is assumed to be fixed at the end in x, y, z directions, therefore it is treated as a cantilever beam. Furthermore, only the tangential force is applied to the beam since the force in y-direction would significantly affect the tool deflection. In addition, the magnitude of the force is 306.4N downward when the depth of cut is 3mm according to Amon Gasagara et al (Gasagara et al., 2019).

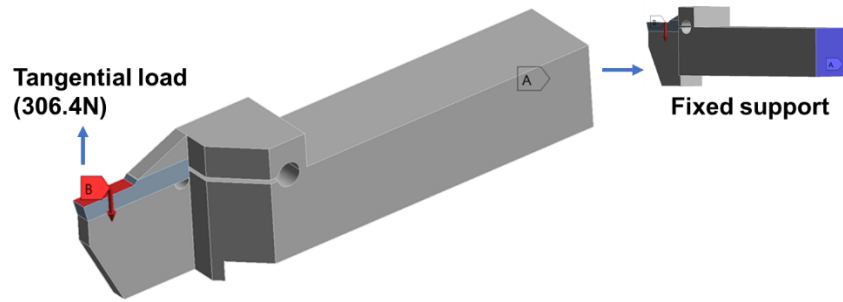


figure 3 Boundary conditions of the model

1.6 SELECTION OF THE MATERIAL PROPERTIES

Tungsten carbide steel and High-speed steel (HSS) have been chosen for the analysed parting tool materials. They are widely used for the materials of lathe tools due to their decent properties. Specific properties are as follows in Table 1. All units are depicted in SI and each property is extracted from the literature and software (Gasagara et al., 2019), (CES Edupack software, 2009).

Table 1 Material properties

Material	Tungsten carbide steel	HSS
Density (kg/m^3)	15,300	8,080
Young's modulus (Pa)	6.0×10^{11}	2.2×10^{11}
Poissons's ratio	0.2	0.25

2. FINITE ELEMENT MODEL

In this section, three finite element models used *Tungsten carbide steel* such as coarse mesh, medium mesh and fine mesh are compared with respect to a mesh convergence study, which verifies whether a good quality of mesh has been chosen. Table 2 indicates the size of elements, number of nodes and elements of each model, respectively. Moreover, we can compare the results of deflection which are shown in figure 5 to figure 7. Each plot has the same scaling factor of the visualisation of the deformation, contour intervals and orientation. As it can be seen in the displacement analyses, similar results come out even though there are significant differences of quantities between each mesh model. Therefore, it can be said that a decent quality of the mesh is selected for the analysis. Accordingly, in section 3, the medium mesh is used to compare the results of finite element deformation analysis since it would be a point of compromise when it comes to accuracy and time-efficiency.

Table 2 Statistics of different mesh models

Mesh	Coarse	Medium	Fine
Size of elements	0.008m	0.0025m	0.0015m
Number of nodes	1277	15680	66457
Number of elements	283	3635	15861

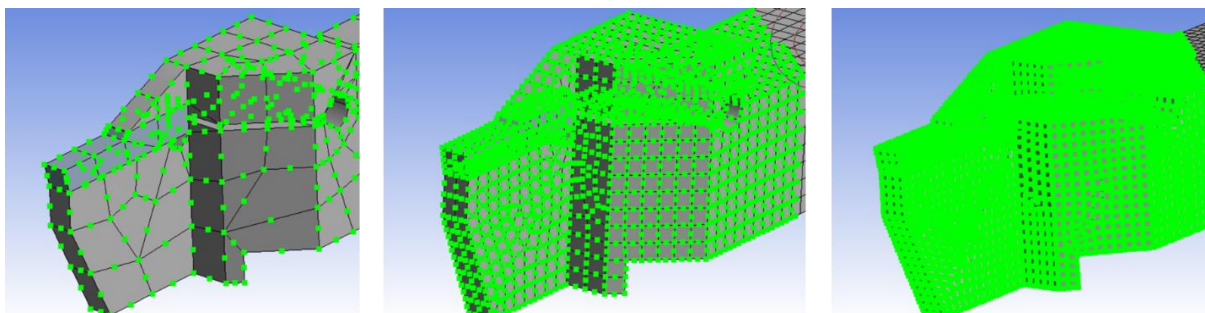


figure 4 Coarse (0.008m), Medium (0.0025m) and Fine (0.0015m) mesh

G: Coarse whole length
 Directional Deformation
 Type: Directional Deformation(Y Axis)
 Unit: m
 Global Coordinate System
 Time: 1 s
 Deformation Scale Factor: 3.1e+002 (Auto Scale)

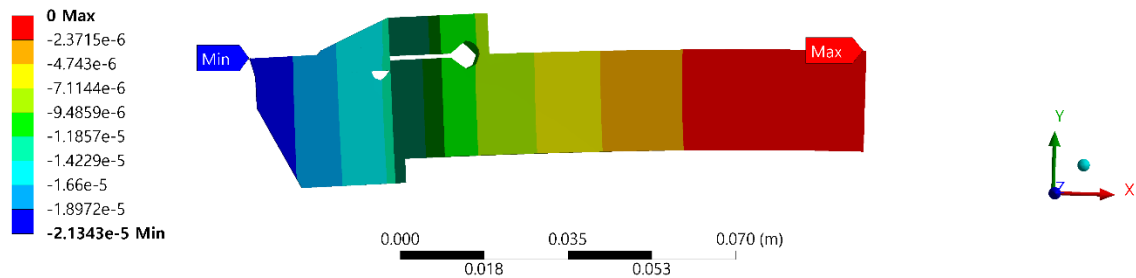


figure 5 Deformation of the model using coarse mesh

H: Medium whole length
 Directional Deformation
 Type: Directional Deformation(Y Axis)
 Unit: m
 Global Coordinate System
 Time: 1 s
 Deformation Scale Factor: 3.1e+002 (Auto Scale)

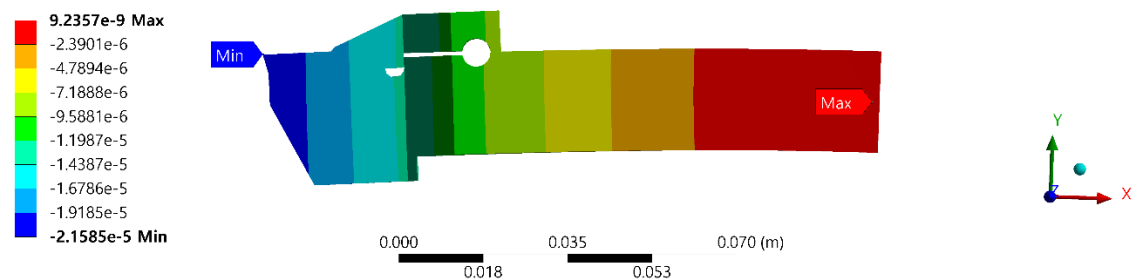


figure 6 Deformation of the model using medium-mesh

A: Whole length fine
 Directional Deformation
 Type: Directional Deformation(Y Axis)
 Unit: m
 Global Coordinate System
 Time: 1 s
 Deformation Scale Factor: 3.1e+002 (Auto Scale)

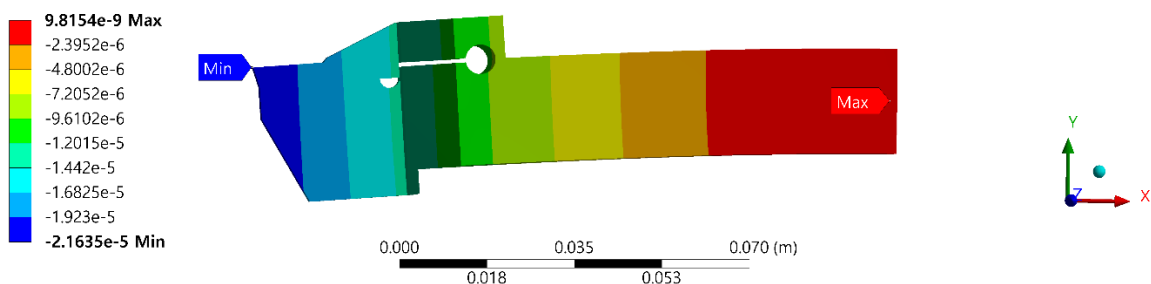


figure 7 Deformation of the model using fine-mesh

3. FINITE ELEMENT RESULTS

When cutting tools are used for the machining process, certain quantities of deflections are inevitably happened in real. Obviously, tool deformations directly affect the accuracy of the outcomes. Thus, two different comparative analyses are carried out in this section to aid engineers in material selection or condition setup. As it is mentioned in the previous section, we compare the tools' deformations. Moreover, not only the comparison between two materials but also the analyses of two cases under different conditions are implemented based on the results of static FEA.

First, the results of the *Tungsten carbide steel* and *HSS* parting tool are indicated in figure 8 and figure 9 which show deformation distribution in the 127mm and 77mm parting tool. As it can be seen in figure 8, the *HSS* parting tool shows bigger deformation (0.0588mm) than the *Tungsten carbide steel* parting tool (0.0216mm). Also, the same trend of the deformation

distribution can be seen in figure 9 which has the maximum results of *HSS* and *Tungsten carbide* as 0.0157mm and 0.0057mm, respectively. As a result, *Tungsten carbide steel* would be recommended to use as a parting tool when it comes to the tool deflection.

Second, figure 10 and figure 11 demonstrate the comparative plots between two cases under different holding conditions. The total length after each tool is held by a holder is 127mm and 77mm, respectively. As it can be seen from the plots, the shorter tool comes out with significantly lower values of the displacement. Accordingly, it is suggested to operate the lathe parting process with a shorter length of the overhang part.

Consequently, based on the comparative deflection analysis results, we recommend using a *Tungsten carbide steel* parting tool rather than *HSS* one and reducing the overhang part by using a tool holder.

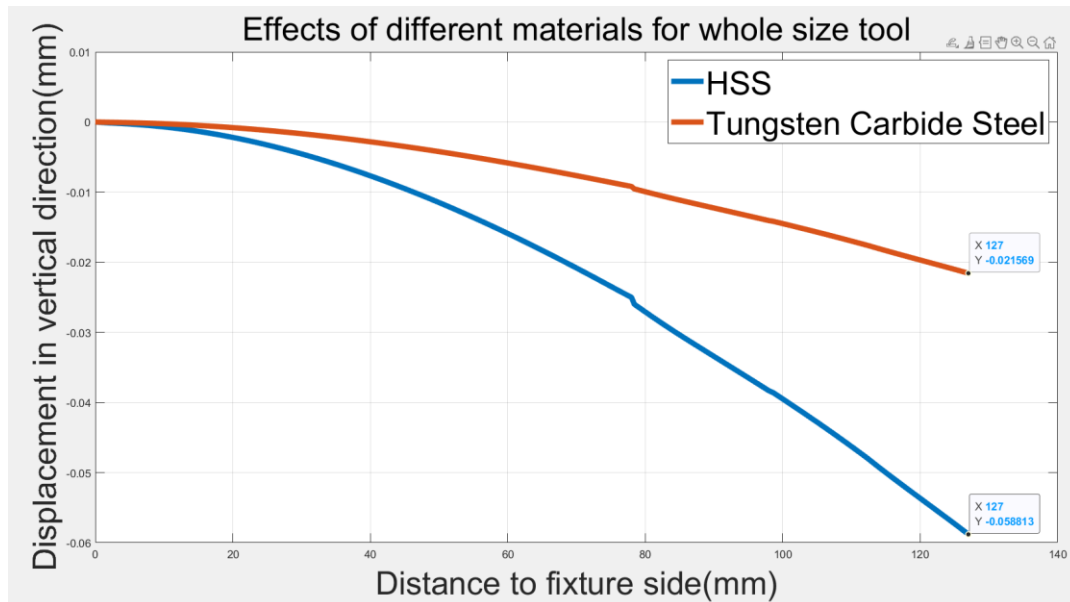


figure 8 Effects of different materials (127mm)

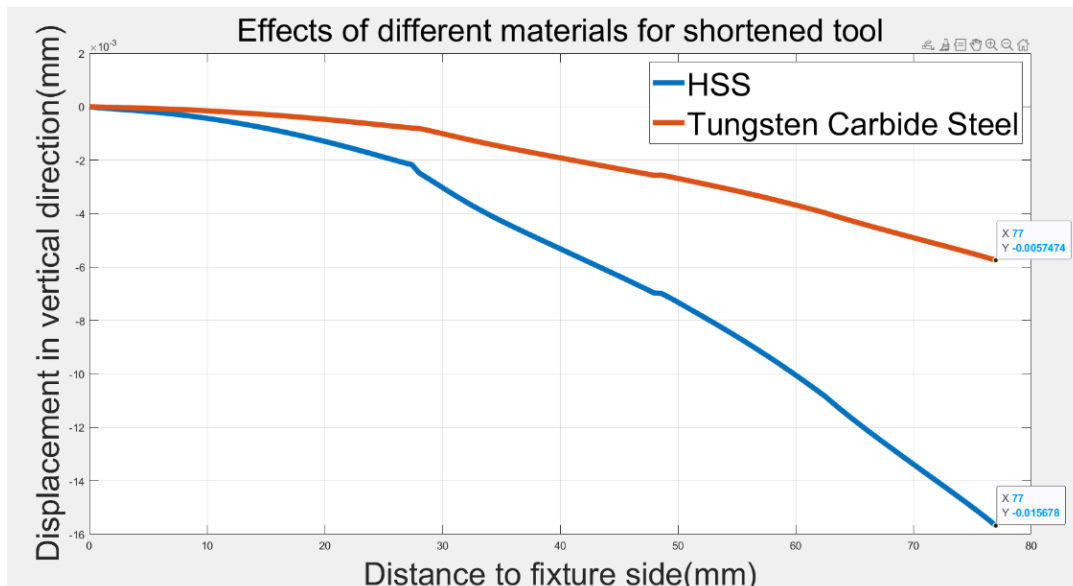


figure 9 Effects of different materials (77mm)

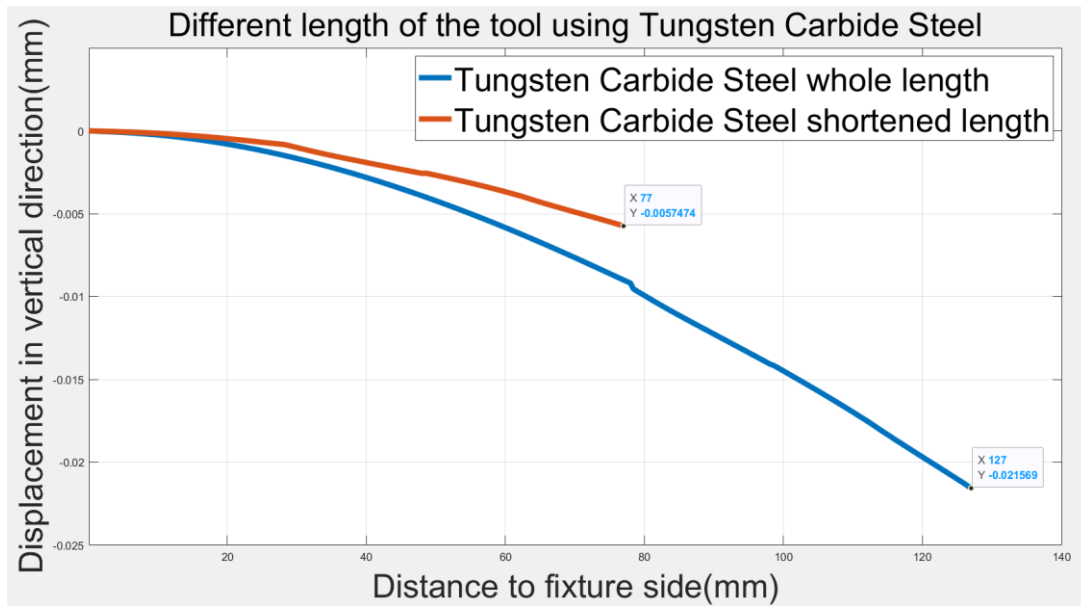


figure 10 Effect of different length (Tungsten carbide steel)

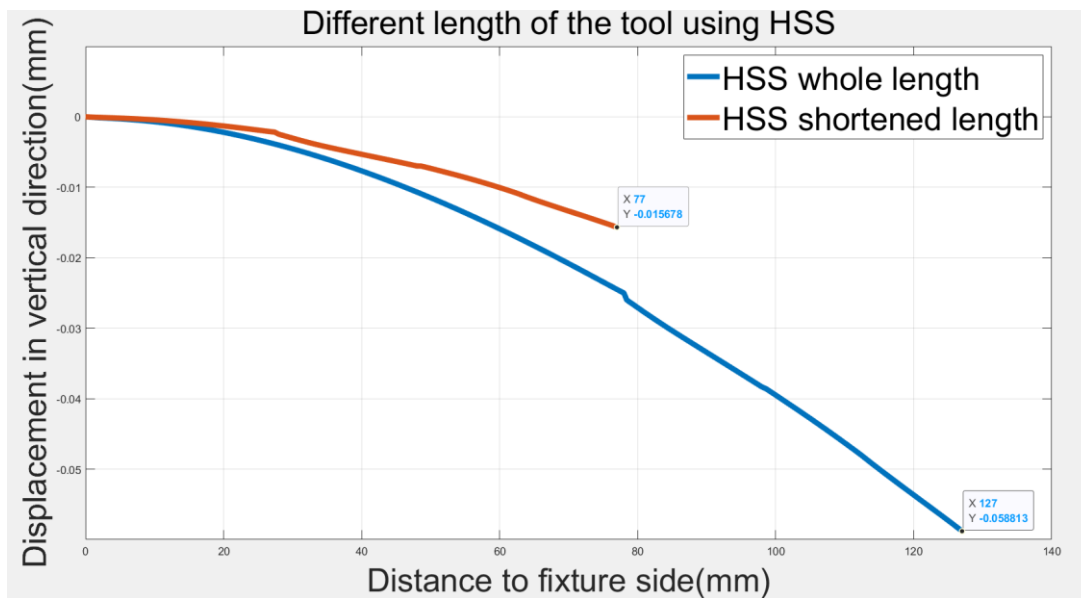


figure 11 Effect of different length (HSS)

4. VALIDATION

For the validation of the simulation results, hand calculation based on the Euler-Bernoulli beam theory is used since the materials are isotropic, the stress-strain relationship is linear and elastic, and static structural analysis is used in this paper. According to figure 2, the idealised geometry is divided into 4 different cross-sections. So, four different second moment of the area of the beam's cross-section is applied to the hand calculation. The specific process of the validation is attached in the Appendix. We compared the values of simulation results and hand calculation results as follows in Table 3. First, simulation results of long parting tools showed significantly high similarity with the theoretical values, which are around 97%. On the other hand, outcomes of short parting tools brought out a relatively low similarity between hand calculation and Ansys results which are around 71%. However, even though they have 74% similarities between each other, the same order of magnitude is demonstrated as can be seen below. Therefore, it can be said that the results of the analysis are reasonable.

Table 3 Validation of simulation results by hand calculation

Analysis type	Tungsten long	Tungsten short	HSS long	HSS short
FEA result (m)	-2.1585×10^{-5}	-5.7688×10^{-6}	-5.8858×10^{-5}	-1.5733×10^{-5}
Theoretical result (m)	-2.0979×10^{-5}	-4.2599×10^{-6}	-5.7216×10^{-5}	-1.1618×10^{-5}
Percentage of theoretical value	97.19%	73.84%	97.21%	73.84%

5. DISCUSSION

According to section 4, the percentage of theoretical value is decreasing as the length of the overhang part is getting smaller. The expected reason for the deviation is as follows:

There are some assumptions when the Euler-Bernoulli beam theory is used, and these assumptions are valid when the length of the beam is much larger than width and height (dimensions of cross-sections) (Bauchau and Craig, 2009). However, as the length of the overhang is getting shorter, the gap between dimensions of the beam is getting smaller therefore, it leads to an inaccurate outcome of hand calculation using the beam theory. Besides that, other factors of inaccuracy are supposed to come out by the complexity of the model such as varied cross-sections and asymmetric geometry. Thus, the benefit of FEA is that if the qualities of the model and mesh are good, it brings more acceptable outcomes no matter how complex or realistic the model is. Moreover, as we have validated the analysis and therefore, we have proven it viable that building a simplified FEA modelling before the experiment can effectively predict the trend of results and hence can substantially aid the experiment design process. However, the limitation of the analysis is the accuracy. The final result obtained through FEA has lost some details and cannot stand alone as the decisive evidence of the complete design due to the neglect of difficult characteristics and the assertion of hypothetical situations. Experiments are still required despite the use of FEA.

Although the static analysis can define the structural deformation or stress distribution efficiently, there are more complicated conditions that will be applied such as vibration, rotation, various directions of loading and so on. Therefore, for more specific solutions to various engineering problems, the dynamic analysis would be required as well. To do so, a number of suggestions can be given as various factors have cared for the selection of materials or set-up.

6. Appendix

Function of bending moment in the beam along the position x

$$M(x) = P(L - x) = EI \frac{d^2 w(x)}{dx^2} \quad \text{Equation (1)}$$

Function of deflection along the position x

$$w(x) = \frac{Px^2}{6EI} (3L - x) + C_1 x + C_2 \quad \text{Equation (2)}$$

Function of slope of the beam along the position x

$$w'(x) = \frac{Px}{2EI} (2L - x) + C_1 \quad \text{Equation (3)}$$

Function of second moment of the beam's cross section

$$I = \frac{bh^3}{12} \quad \text{Equation (4)}$$

$b = \text{width of the cross section,}$

$E = \text{Young's modulus,}$

$h = \text{height of the cross section,}$

$L = \text{length of the beam,}$

$x = \text{position on the beam,}$

$C_1, C_2 = \text{Constants of integration}$

These functions are defined by being applied to each cross-section.

7. References

- BAUCHAU, O. A. & CRAIG, J. I. 2009. Euler-Bernoulli beam theory. *Structural analysis*. Springer.
- BENZLEY, S. E., PERRY, E., MERKLEY, K., CLARK, B. & SJAARDAMA, G. A comparison of all hexagonal and all tetrahedral finite element meshes for elastic and elasto-plastic analysis. Proceedings, 4th international meshing roundtable, 1995. Citeseer, 179-191.
- Camuz, S., Söderberg, R., Wärmefjord, K. and Lundblad, M., 2018. Tolerance Analysis of Surface-to-Surface Contacts Using Finite Element Analysis. *Procedia CIRP*, 75, pp.250-255.
- CES EduPack software, Granta Design Limited, Cambridge, UK, 2009.
- GASAGARA, A., JIN, W. & UWIMBABAZI, A. 2019. Stability analysis for a single-point cutting tool deflection in turning operation. *Advances in Mechanical Engineering*, 11, 1687814019853188.
- MADIREDDY, J. 2014. Importance of Lathe Machine in Engineering Field and its usage. *Global Journal of Research In Engineering*.
- What are the Types of Elements Used in FEA?, 2019. . Enterfea. URL <https://enterfea.com/what-are-the-types-of-elements-used-in-fea/> (accessed 11.18.21).